

Exact diagonalization study of the tunable edge magnetism in graphene

David J. Luitz and Fakher F. Assaad
*Institute for Theoretical Physics and Astrophysics,
University of Würzburg, Am Hubland, 97074 Würzburg, Germany*

Manuel J. Schmidt
Department of Physics, University of Basel, Klingelbergstrasse 82, 4056 Basel, Switzerland
(Dated: August 1, 2018)

The tunable magnetism at graphene edges with lengths of up to 48 unit cells is analyzed by an exact diagonalization technique. For this we use a generalized interacting one-dimensional model which can be tuned continuously from a limit describing graphene zigzag edge states with a ferromagnetic phase, to a limit equivalent to a Hubbard chain, which does not allow ferromagnetism. This analysis sheds light onto the question why the edge states have a ferromagnetic ground state, while a usual one-dimensional metal does not. Essentially we find that there are two important features of edge states: (a) umklapp processes are completely forbidden for edge states; this allows a spin-polarized ground state. (b) the strong momentum dependence of the effective interaction vertex for edge states gives rise to a regime of partial spin-polarization and a second order phase transition between a standard paramagnetic Luttinger liquid and ferromagnetic Luttinger liquid.

PACS numbers: 73.21.-b,75.70.Rf,81.05.ue,73.22.Pr

I. INTRODUCTION

Since it has first been isolated in the laboratory,¹ graphene, a two-dimensional honeycomb lattice of carbon atoms,² attracts much attention. In fact, graphene has multiple amazing properties. To name only a few of them, it ranges among the mechanically strongest materials,³ it shows a quantum Hall effect at room temperature,⁴ and, due to its unusual Dirac band structure, it allows the study of relativistic quantum physics in a solid state environment.⁵ Furthermore, its potential application as the basis of the next generation of electronic devices stimulated great efforts to gain experimental control as well as theoretical understanding of this astonishing material.

Usually a strong electron confinement increases the strength of electron-electron interactions by pushing the electrons close together. However, in spite of the extreme electron confinement to only one single layer of atoms, many experiments in graphene may be explained by assuming the electrons to be non-interacting. This is especially true for experiments probing the bulk properties of graphene, as the bulk density of states vanishes at the Fermi level, suppressing the manifestation of interaction effects. On the other hand, the properties of zigzag edges differ greatly from the bulk properties. So-called edge states, i.e. one-dimensional states with very small bandwidth, localized at these edges, give rise to a peak in the local density of states at the Fermi energy.⁶ The enhanced density of states allows the electron-electron interaction to drive the zigzag edges to a ferromagnetic state with a magnetic moment localized at the edge.⁷⁻¹² This phenomenon is known as edge magnetism.

At normal graphene edges the electron-electron interaction is so strong and the bandwidth of the edge states is so small that the spins of all electrons in the edge states

are completely aligned. However, as has been proposed recently, graphene/graphane interfaces provide means to tune the bandwidth of the edge states to regimes in which the edge starts to depolarize and the edge magnetism is gradually suppressed until, for a critical edge state bandwidth, the magnetism disappears.¹³

In Ref. 13 it was argued that this interaction-induced magnetism can be understood on the basis of an effective model, describing the interacting one-dimensional edge states only, while the bulk states are neglected. What at first glance appears to be a contradiction to the Lieb-Mattis theorem,¹⁴ stating that the ground state of interacting electrons in one dimension cannot be spin polarized, can be resolved by noting that the effective edge state model does not fulfill the prerequisites of the Lieb-Mattis theorem.¹³ The deeper reasons for the existence of a ferromagnetic ground state in a one-dimensional interacting electron system, however, remained elusive. The present work is devoted to this issue.

In this paper we present a systematic exact diagonalization analysis of interacting edge states. Two striking features of edge states turn out to be most important for their magnetic properties: (a) the edge states exist only in a restricted part of the Brillouin zone and (b) the transverse edge state wave function has a strong characteristic momentum dependence. These features have consequences for the effective low-energy theory, namely (a) *no umklapp processes are allowed in the interaction Hamiltonian* and (b) *the interaction vertex acquires an unusually strong momentum dependence*. In order to be able to study the consequences of these two features, we introduce a generalized model in which we add an artificial interaction term describing umklapp processes and allow the momentum-dependence of the interaction vertex to be tuned from a momentum-independent vertex, as in usual metals, to the full momentum-dependence,

as it is found in edge states. Therefore, the generalized model can be tuned continuously from the limit in which it describes edge states to a limit which corresponds to usual one-dimensional metals such as the Hubbard chain. We solve this generalized model for graphene zigzag edges of finite length $L = 48$ unit cells (i.e. ~ 12 nm) by exact diagonalization using the Lanczos method for the determination of the ground state of the effective model.^{15–18}

The paper is organized as follows. In Sec. II we review the direct model as it has been derived in Ref. 13 and introduce the more versatile generalized model with additional tunability. In Sec. III the exact diagonalization analysis of the generalized model is presented. Finally, the results are discussed in Sec. IV.

II. EDGE STATE MODELS

In this section we introduce the models on which our analysis is based. The edge state model obtained from the direct projection of the honeycomb lattice Hubbard model to the Fock space spanned only by the edge states has been discussed in Ref. 13. This model will be called the *direct model* in the following. We identify two important features of the direct model: (a) the restriction of the Brillouin zone for the edge states and (b) the strong dependence of the transverse localization length on the momentum along the edge. After having analyzed the consequences of these features for the effective interaction vertex, we propose a generalized edge state model in which these features can be tuned. This allows us to investigate the impact of each of these edge state features on the magnetic properties. In particular, the generalized model can be tuned continuously from a Hubbard chain limit, i.e., a usual one-dimensional metal without any ferromagnetic ground state, to the edge state limit with its ferromagnetic ground state.

A. Direct derivation from the honeycomb model

We start from the simplest possible non-interacting tight-binding model of electrons in graphene zigzag ribbons, taking into account only nearest neighbor hoppings of π electrons $\mathcal{H} = \sum_{\langle i,j \rangle, \sigma} c_{i\sigma}^\dagger c_{j\sigma}$, where $\langle i,j \rangle$ runs over nearest neighbor sites of a half-infinite honeycomb lattice, $i \equiv (m, n, s)$ is a collective site index for the (m, n) th unit cell and the $s = A, B$ sublattice (see Fig. 1), and $c_{i\sigma}$ annihilates an electron at site i with spin σ . Since we are exclusively interested in the zero energy eigenstates of \mathcal{H} , the actual energy scale of \mathcal{H} is unimportant so that we may drop it.¹⁹ The zero energy states are created by the fermionic edge state operator

$$e_{p\sigma}^\dagger = \sum_n \psi_p(n) c_{pn\sigma}^\dagger, \quad \psi_p(n) = \mathcal{N}_p u_p^n \quad (1)$$

where $u_p = -1 - e^{ip}$, p is the momentum in m direction (along the edge), and $c_{pn\sigma} = L^{-\frac{1}{2}} \sum_m e^{-ipm} c_{(m,n,B)\sigma}$,

with the number of unit cells L in m direction, i.e., along the edge. The p -dependent normalization constant $\mathcal{N}_p = \sqrt{2 \cos(p - \pi) - 1}$ can be interpreted as the weight of the edge state wave function right at the edge atoms where $n = 0$. It is easily seen that $\mathcal{H} e_{p\sigma}^\dagger = 0$. As the edge state wave function is only non-zero on the B sublattice we omit the sublattice index, setting it to $s = B$.

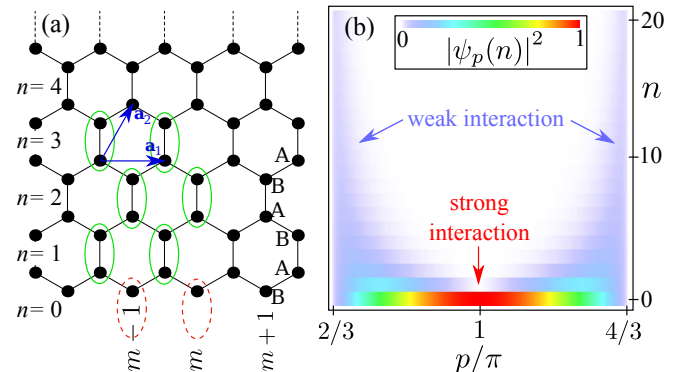


FIG. 1. (Color online) Part (a) shows the half-infinite honeycomb lattice. The solid ellipses (green) are the complete unit cells in the bulk region and the dashed ellipses indicate the cut unit cells at the α edge. The n and m directions are indicated as well as the sublattice indices A, B. Part (b) shows the modulus square of the transverse (in n direction) edge state wave function $|\psi_p(n)|^2$ on the B sublattice sites in the reduced Brillouin zone $\frac{2\pi}{3} \leq p \leq \frac{4\pi}{3}$. The extreme momentum dependence of the localization of ψ_p in n direction is crucial for the magnetic properties of edge states.

The two most important features of the edge state wave function [Eq. (1)] are: (a) The edge state only exists for momenta $\frac{2\pi}{3} < p < \frac{4\pi}{3}$. In the rest of the Brillouin zone the edge state wave function is not normalizable, as $|u_p| > 1$ for these momenta. (b) In n direction the edge state is sharply localized at the edge for $p = \pi$, whereas for p close to one of the Dirac points $K = \frac{2\pi}{3}$ and $K' = \frac{4\pi}{3}$, the wave function delocalizes into the bulk [see also Fig. 1(b)]. These two edge state properties are stable against adding more details, such as second-nearest neighbor hopping or various edge passivations, to the honeycomb Hamiltonian \mathcal{H} .^{13,20} The detailed analysis presented in this paper will clarify that *the existence of edge magnetism and in particular its tunability are consequences of these two edge state properties*.

The p -dependence of the localization length of ψ_p has consequences for the edge states' self-energy ϵ_0 as well as for their interaction vertex function Γ . Neglecting the bulk state contributions,¹³ the self-energy correction due to a perturbation V , which is invariant along the edge, is given by $\epsilon_0(p) = \langle \psi_p | V | \psi_p \rangle$. Due to the delocalization of $\psi_p(n)$ for p near K, K' , edge-localized perturbations V lead to self-energy corrections for which $\epsilon_0(K) = \epsilon_0(K') = 0$ while $\epsilon_0(\pi) \sim \|V\|$. For sufficiently well behaved perturbations the self-energy correction gives rise to a smooth edge state energy dispersion with a bandwidth $\Delta \sim \|V\|$. For a large class of these

edge-localized perturbations, the self-energy correction approximately has the form

$$\epsilon_0(p) \simeq \mathcal{N}_p^2 \Delta, \quad (2)$$

with \mathcal{N}_p^2 the p -dependent weight of the edge state wave function right at the edge. Eq. (2) expresses that an edge state which is more localized at the edge experiences a stronger self-energy correction from an edge-localized perturbation than an edge state which is delocalized into the bulk region. Examples of such perturbations are edge passivations, graphane termination,²⁰ or local interactions with the substrate. Note that the edge state bandwidth Δ is experimentally tunable in various ways so that we consider Δ as a free parameter. Therefore, the noninteracting part of the direct model (dm) edge state Hamiltonian is given by:

$$H_0^{\text{dm}} = -\Delta \sum_{\sigma} \sum_p' \mathcal{N}_p^2 e_{p,\sigma}^{\dagger} e_{p,\sigma}, \quad (3)$$

where the sum is restricted such that only edge state operators $e_{p\sigma}$ with $\frac{2\pi}{3} \leq p \leq \frac{4\pi}{3}$ appear.

The effective interaction of the edge states, derived by projecting the Hubbard Hamiltonian on the two-dimensional honeycomb lattice $H_U = U \sum_i c_{i\uparrow}^{\dagger} c_{i\uparrow} c_{i\downarrow}^{\dagger} c_{i\downarrow}$ to the Fock space spanned by the edge states, reads¹³

$$H_1^{\text{dm}} = \frac{U}{L} \sum_{p,p',q}' \Gamma(p,p',q) e_{p+q\uparrow}^{\dagger} e_{p\uparrow} e_{p'-q\downarrow}^{\dagger} e_{p'\downarrow}. \quad (4)$$

Together, we have the effective Hamiltonian $H^{\text{dm}} = H_0^{\text{dm}} + H_1^{\text{dm}}$. The interaction vertex is given by the overlap of the wave functions of all four fermions (with momenta $p+q, p, p'-q, p'$) participating in the interaction

$$\begin{aligned} \Gamma(p,p',q) &= \sum_{n=0}^{\infty} \psi_{p+q}^*(n) \psi_p(n) \psi_{p'-q}^*(n) \psi_{p'}(n) \\ &= \frac{\mathcal{N}_{p+q} \mathcal{N}_p \mathcal{N}_{p'-q} \mathcal{N}_{p'}}{1 - u_{p+q}^* u_p u_{p'-q}^* u_{p'}}. \end{aligned} \quad (5)$$

While the denominator, resulting from the geometric series over n , turns out to lead only to unimportant quantitative corrections, the numerator of Γ , which is the product of the wave function weights at the edge \mathcal{N}_p for each of the four fermion operators, leads to the momentum-dependence of the interaction strength which is important for the stability of the weak edge magnetism. Essentially, the effective interaction becomes stronger the more localized the participating fermions are, i.e., the closer their momenta are to $p = \pi$. If one or more of the momenta are close to the Dirac points $\frac{2\pi}{3}, \frac{4\pi}{3}$, where the edge state wave functions delocalize into the bulk, the effective interaction is suppressed (see Fig. 1). Note that setting the denominator in Eq. (5) to unity corresponds to assuming that the Hubbard interaction is only present at the outermost line of carbon atoms right at the edge.

Such an approximation has been used in Ref. 21. We find that this approximation is inessential for the edge magnetism, leading only to quantitative corrections.

An important consequence of the restriction of the p summation in Eq. (4) is the *absence of umklapp processes*. As explained above, edge states only exist in one third of the Brillouin zone, i.e. for $\frac{2\pi}{3} \leq p \leq \frac{4\pi}{3}$, so that no four fermion process with momentum $\pm 2\pi$ exists. Indeed, within the restricted Brillouin zone, the process with the largest possible total momentum p_{tot} is $e_{4\pi/3\uparrow}^{\dagger} e_{2\pi/3\uparrow} e_{4\pi/3\downarrow}^{\dagger} e_{2\pi/3\downarrow}$, i.e. $p_{\text{tot}} = \frac{4\pi}{3} < 2\pi$. Processes with larger total momentum leave the restricted Brillouin zone and are therefore suppressed, as they involve the overlap of edge states and bulk states, which is small. Also, most of the bulk states live in a different energy regime than the edge states.¹³

Thus, we have identified two properties of edge states which make them fundamentally different from usual one-dimensional conductors:

- (a) Due to the restricted Brillouin zone, umklapp processes are forbidden.
- (b) The transverse localization \mathcal{N}_p of the edge state wave function gives rise to a tunable band width $\epsilon_0(p) \simeq \mathcal{N}_p^2 \Delta$. Furthermore, the interaction vertex becomes weaker if the momenta of the participating fermions approach a Dirac point, i.e. $\Gamma(p,p',q) \propto \mathcal{N}_{p+q} \mathcal{N}_p \mathcal{N}_{p'-q} \mathcal{N}_{p'}$.

We will show that these properties are the basis for the magnetism at graphene edges.

B. Generalized model

We now introduce a generalized model in which the different aspects of the effective electron-electron interaction, found in the previous subsection, may be tuned independently. For this, we map the edge state operators $e_{p,\sigma}$ which correspond to right (left) moving modes for $\pi < p < \frac{4\pi}{3}$ ($\frac{2\pi}{3} < p < \pi$), to fermionic operators $c_{kr\sigma}$ in which $r = R, L$ specifies the direction of motion and $-\frac{\pi}{6} \leq k \leq \frac{\pi}{6}$, i.e. $c_{kr\sigma} = e_{k+\pi+r\pi/6,\sigma}$ and $p = k + \pi + r\pi/6$. The direction of motion $r = R, L$ corresponds to $r = \pm 1$ when used in formulas. Note that the zero point of k has been shifted so that $k = 0$ corresponds to $p = \pi \pm \pi/6$ for right and left movers, respectively (see Fig. 2).

For the non-interacting part of the generalized edge state model we assume a linear spectrum with slope $\pm v_F$

$$H_0 = v_F \sum_{\substack{r=R,L \\ \sigma=\uparrow,\downarrow}} \sum_{k=-\pi/6}^{\pi/6} (rk) c_{kr\sigma}^{\dagger} c_{kr\sigma}. \quad (6)$$

This linearization of the self-energy [Eq. (2)] only leads to inessential quantitative corrections (see also Appendix B).

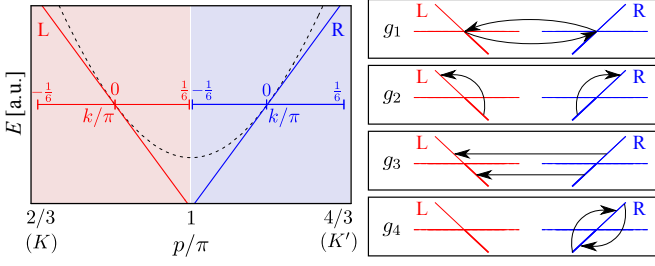


FIG. 2. (Color online) Left: The self-energy $\sim \mathcal{N}_p^2$ of the direct model (dashed line) and the linearized self-energy (solid lines). Right: The four possible interaction processes. The g_3 process is not allowed for graphene edge states.

The partitioning into left- and right-movers always gives rise to four terms in the interaction part H_1 of the Hamiltonian involving different combinations of left- and right-moving modes. Conventionally, these terms are called g_1, g_2, g_3, g_4 processes (see Fig. 2 and Ref. 22). g_2, g_4 correspond to forward scattering, involving processes that scatter only between modes with the same direction of motion, g_1 refers to backward scattering, and g_3 are the umklapp terms which are forbidden in edge states. Note that, unlike in usual g -ology,²² we may not assume that the coupling constants for the individual g_i processes are constant. The momentum-dependence of the g_i must be taken into account.

The two forward scattering processes g_2 and g_4 may be merged together into one Hamiltonian²³

$$H_1^{\text{fs}} = \frac{U}{L} \sum_{r,r'} \sum_{k,k',q} S_{k+q}^r S_k^r S_{k'-q}^{r'} S_{k'}^{r'} \times \\ : c_{k+qr}^\dagger c_{kr} c_{k'-qr'}^\dagger c_{k'r'} : , \quad (7)$$

where $: A :$ enforces the normal order²² of the operator A . The primed sum is restricted such that $|k| < \pi/6$ for all momentum arguments k in the electron operators. In order to be able to change the amplitude of the momentum-dependence of the interaction vertex $\Gamma(p, p', q)$ [see Eq. (5)], we introduce the factors

$$S_k^r = \sqrt{1 - r\Gamma_1 k}, \quad (8)$$

from which we build the interaction vertex for the generalized model. The factor $\Gamma_1 \in [0, 6/\pi]$ quantifies the momentum-dependence. For $\Gamma_1 = 0$ the interaction is momentum-independent. This limit corresponds to usual one-dimensional Hubbard chains. For $\Gamma_1 = 6/\pi$ the interaction goes to zero if at least one of the fermions is close to the upper band edge ($k = r\pi/6$). This corresponds to the direct model, where the trigonometric term under the square root in \mathcal{N}_p has been replaced by a linear approximation. The differences between the generalized model in the edge state limit and the direct model only lead to quantitative renormalizations of the critical point, as shown in Appendix B. The essential property of the interaction vertex is that it approaches zero if one

of the fermion momenta gets close to the Dirac points. This feature is present in the direct and in the generalized model with $\Gamma_1 = 6/\pi$.

The form of the backscattering (g_1) Hamiltonian H_1^{bs} is similar to H_1^{fs} . However the scattering takes place between left- and right-movers

$$H_1^{\text{bs}} = \lambda_{\text{bs}} \frac{U}{L} \sum_r \sum_{k,k',q} S_{k+q}^r S_k^{-r} S_{k'-q}^{-r} S_{k'}^r \times \\ c_{k+q,r,\uparrow}^\dagger c_{k,-r,\uparrow} c_{k'-q,-r,\downarrow}^\dagger c_{k',r,\downarrow}. \quad (9)$$

We have introduced the additional parameter λ_{bs} which allows us to tune the overall strength of the g_1 processes relative to the g_2, g_4 processes. $\lambda_{\text{bs}} = 1$ corresponds to the physical backscattering strength which is required by SU(2) invariance.²² Nevertheless, we will investigate the consequences of a suppression of backscattering since this will be important for a bosonization analysis of the generalized model which will be presented in an upcoming paper.²⁴

As already pointed out, an important feature of edge states is the absence of umklapp processes in the effective electron-electron interaction. However, in order to be able to compare the edge state model to a Hubbard chain, we add an artificial umklapp process with relative strength λ_{us} to the Hamiltonian of the generalized model

$$H_1^{\text{us}} = \lambda_{\text{us}} \frac{U}{L} \sum_r \sum_{k,k',q} S_{k+q}^r S_k^{-r} S_{k'-q}^{-r} S_{k'}^{-r} \times \\ c_{k+q,r,\uparrow}^\dagger c_{k,-r,\uparrow} c_{k'-q,r,\downarrow}^\dagger c_{k',-r,\downarrow}. \quad (10)$$

Varying λ_{us} between 1 (Hubbard chain limit) and 0 (edge state limit) allows us to investigate the consequences of the presence of umklapp processes for one-dimensional ferromagnetism.

Alltogether, the four parameters v_F/U , λ_{bs} , λ_{us} , and Γ_1 define the phase space of the generalized model

$$H = H_0 + H_1^{\text{fs}} + H_1^{\text{bs}} + H_1^{\text{us}}. \quad (11)$$

The following limits of this model may be identified:

1. Edge state limit: the generalized model with the parameters $\lambda_{\text{bs}} = 1$, $\lambda_{\text{us}} = 0$, and $\Gamma_1 = 6/\pi$, is a good approximation of the direct model.
2. Hubbard chain limit: for $\lambda_{\text{bs}} = 1$, $\lambda_{\text{us}} = 1$, and $\Gamma_1 = 0$, the generalized model essentially describes a one-dimensional Hubbard chain. The only difference is the assumption of a linearized single-particle spectrum instead of the $2 \cos(k)$ dispersion.

Note that it is important to work in the k -space formulation because it is difficult to control the umklapp scattering or the momentum dependence of the interaction vertex in a real space formulation. One reason for this is that an interaction vertex $\Gamma(p, p', q)$ with a non-trivial p, p' dependence does not transform to a real space interaction of the form $V(x - x')$ but to a complicated non-local interaction. This also hampers the application of DMRG methods to this problem.

III. EXACT DIAGONALIZATION

The ground state of the generalized model is calculated for finite sized zigzag edges up to $L = 48$ by the Lanczos exact diagonalization method²⁵⁻¹⁸. The magnetic properties of the ground state depend on the ratio between the kinetic energy and the potential energy $v_F\pi/U$, which is experimentally tunable at graphene/graphane interfaces.¹³ Three additional tuning parameters $\Gamma_1, \lambda_{\text{us}}, \lambda_{\text{bs}}$, which are not accessible experimentally, have been added in order to be able to study the significance of the momentum dependence of the interaction vertex (Γ_1), the influence of the absence of umklapp scattering (λ_{us}) in edge states, and also the importance of backscattering (λ_{bs}). With those artificial parameters, the generalized model may be tuned continuously from a Hubbard chain limit to the edge state limit. In both limits the model describes an interacting one-dimensional metal. The magnetic properties in these two limits, however, differ strongly: while the usual Hubbard chain (with umklapp scattering and without momentum dependence) does not give rise to a ferromagnetic ground state, the edge states (without umklapp scattering and with momentum-dependent interactions) show two magnetic phases in addition to the non-magnetic Luttinger liquid phase: for strong interactions the saturated edge magnetism⁷⁻⁹ is recovered, while for intermediate interaction strengths, a ferromagnetic Luttinger liquid appears.

The Hamiltonian H [Eq. (11)] conserves the numbers N_\uparrow, N_\downarrow of up-spin and down-spin electrons, so that H is block diagonal in the S_z subspaces, which we define by the total spin-polarization in z direction

$$S_z = \frac{1}{2}(N_\uparrow - N_\downarrow) = 0, 1, 2, \dots, N/2. \quad (12)$$

The total number of electrons $N = N_\uparrow + N_\downarrow = L/3$ is kept constant. This corresponds to half-filling. Note, however, that the filling is physically relevant only if umklapp scattering is present (i.e. $\lambda_{\text{us}} > 0$). For the edge states in which we are finally interested, umklapp scattering is forbidden so that the filling is irrelevant as it only leads to quantitative renormalizations of the interaction strength and the Fermi velocity. In the following, we determine the ground state of H in each S_z subspace separately.

Note that by the definition of the S_z subspaces we have chosen a spin quantization axis. The Hamiltonian H , however, is $SU(2)$ symmetric if the backscattering is at its physical strength $\lambda_{\text{bs}} = 1$. Furthermore, since we are dealing with finite systems, there will be no spontaneous rotational symmetry breaking. Thus, edge magnetism will become manifest in a $(2S+1)$ -fold ground state degeneracy, corresponding to a high spin (S) state. For instance, if in a system with $N = 2$ electrons the lowest energy states in the subspaces $S_z = -1, 0, 1$ are the degenerate ground states, then the $\frac{1}{2}$ spins of two electrons point into the same direction, building an $S = 1$ super spin. Because the $SU(2)$ symmetry of the individ-

ual electron spins is not broken, also this composite super spin has full rotational symmetry. The S_z quantum numbers of the degenerate S_z subspaces then correspond to the magnetization of this composite spin system. Note that the spin-orbit interaction lowers the symmetry of the super spin, as it breaks the $SU(2)$ invariance of the individual electron spins which form the super spin.

For practical reasons, we extract the total spin quantum number S of the ground state from its ground state degeneracy $(2S+1)$, which is obtained from the S_z subspace ground state energies. We have checked that this is equivalent to calculating the total spin S of the ground state directly.

A. Hubbard chain vs. edge states

First we study the crossover from a usual Hubbard chain to interacting edge states. As explained above, the generalized model can be tuned continuously between these two limiting cases by means of the parameters λ_{us} and Γ_1 . We postpone the analysis of backscattering to the next subsection and set $\lambda_{\text{bs}} = 1$ here.

It is most instructive to begin with the Hubbard chain limit of the generalized model, which is characterized by the full umklapp process strength $\lambda_{\text{us}} = 1$ and a suppressed momentum dependence of the interaction $\Gamma_1 = 0$. With this parameter set the direct model resembles a one-dimensional metal with a linear single particle dispersion instead of a cos-dispersion.²⁶ The lowest eigen energies in the different S_z subspaces for the parameter set described above are shown in Fig. 3. Obviously, the ground state is non-degenerate and resides in the $S_z = 0$ subspace for arbitrary $v_F\pi/U$, except for the limit of infinitely large U . Thus, as expected, no ferromagnetic phase transition exists for the Hubbard chain limit of the generalized model at finite $v_F\pi/U$, in consistence with the Lieb-Mattis theorem¹⁴ which states that the ground state of a system of one-dimensional interacting electrons has zero total spin and is non-degenerate with higher spin subspaces.²⁷

Next, the generalized model is tuned away from the Hubbard chain limit by suppressing the umklapp scattering $\lambda_{\text{us}} < 1$. Suppressed umklapp scattering is one of the properties of edge states which makes them fundamentally different from usual one-dimensional metals. In the inset of Fig. 3, the lowest eigen energies of the $S_z = 0$ and the $S_z = \pm N/2$ (full spin-polarization) subspaces are shown as λ_{us} is reduced from 1 to 0 in steps of 0.2. For any $\lambda_{\text{us}} < 1$ there is a nonzero critical value for $v_F\pi/U$ below which the lowest energy states of these two subspaces and also for all S_z in between (not shown in the inset of Fig. 3) are equal. This corresponds to a high spin state of size $S = 6$ in which the spins of all electrons point into the same direction. The critical point at which the transition between $S = 0$ and $S = N/2$ takes place

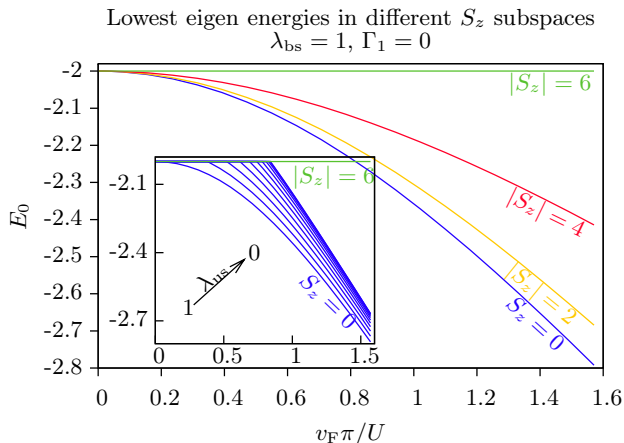


FIG. 3. (Color online) Lowest eigen energies in different S_z subspaces for $N = 12$ in the Hubbard limit with $\lambda_{bs} = 1$, $\lambda_{us} = 1$, $\Gamma_1 = 0$, and $U = 1$. The inset shows the lowest eigen energies of the $S_z = 0, 6$ subspaces (zero and full spin-polarization) as the umklapp scattering is suppressed. The lower lines correspond to $\lambda_{us} = 1$ and the higher lines to $\lambda_{us} = 0$. For the lines in between, λ_{us} decreases in steps of 0.2.

depends on the umklapp scattering strength

$$\left[\frac{v_F \pi}{U} \right]_{\text{crit.}}^{(\Gamma_1=0)} \propto (1 - \lambda_{us})^y. \quad (13)$$

For $N = 12$ we find for the exponent $y \simeq 0.5 \pm 0.02$. Obviously, the absence of umklapp scattering allows a high spin ground state. However, for $\lambda_{us} < 1$ and $\Gamma_1 = 0$, the system instantly jumps from zero polarization $S = 0$ to the maximal possible polarization $S = N/2$ at the critical point $[v_F \pi / U]_{\text{crit.}}^{(\Gamma_1=0)}$. This is a first order phase transition. For the case of completely suppressed umklapp scattering $\lambda_{us} = 0$ this is shown in Fig. 4 (a), where the lowest eigen energies of all subspaces are plotted as a function of $v_F \pi / U$: the $S_z = 0$ subspace contains the non-degenerate ground state until at the critical point the lowest energy eigenstates of *all* subspaces form the degenerate ground state; no intermediate regime of $v_F \pi / U$ exists in which there is only a degeneracy between some of the S_z subspaces.

The reason for the instant jump in the total spin is as follows: once the Stoner criterion $v_F \pi / U > [v_F \pi / U]_{\text{crit.}}^{(\Gamma_1=0)}$ is met, the interaction energy gain $\delta E_U(S)$ associated with developing a certain spin polarization S is larger than the corresponding kinetic energy penalty $\delta E_{\text{kin}}(S)$. Unlike in two or three dimensions, however, for one-dimensional systems with momentum-independent interactions, $\delta E(S) = \delta E_U(S) + \delta E_{\text{kin}}(S)$ has no minimum, i.e. $\delta E(S+1) < \delta E(S)$, for all $S < S_{\text{max}}$. Thus, the system instantly ‘flows’ to the highest possible polarization S_{max} , once the Stoner criterion is met. This is a rather common feature of one-dimensional systems with a constant interaction vertex (such as the Hubbard

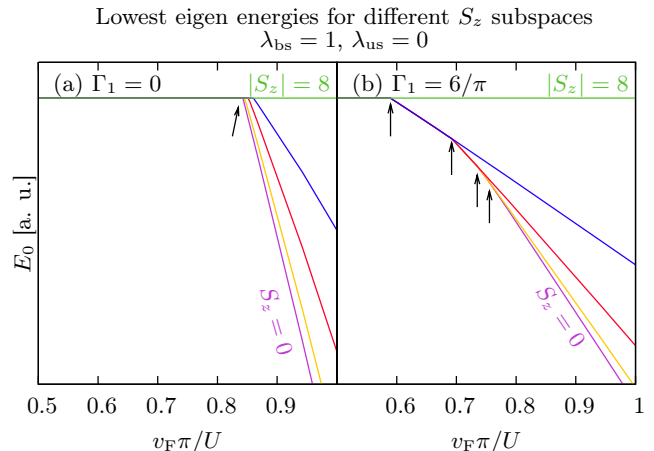


FIG. 4. (Color online) Lowest eigen energies with completely suppressed umklapp scattering $\lambda_{us} = 0$ and different momentum-dependencies Γ_1 . Furthermore, $N = 16$, $\lambda_{bs} = 1$, and $U = 1$. Part (a) shows the case of a momentum-independent interaction vertex ($\Gamma_1 = 0$), where the ground state degeneracy jumps from 17 ($= 2S_{\text{max}} + 1$) directly to 1 at the position indicated by the arrow. Part (b) shows the case of an interaction vertex with maximal momentum-dependence $\Gamma_1 = 6/\pi$. The arrows indicate a change in the ground state degeneracy.

interaction) and can easily be observed in a variational calculation of the ground state properties (see Appendix A).

The momentum-dependence of the interaction vertex ($\Gamma_1 > 0$) reduces the interaction energy gain as the spin-polarization S becomes larger. This is because for larger S , the Fermi level of the spin-up right-movers is shifted to higher momenta where the interaction is suppressed by the $S_k^{r=R}$ factors [see Eq. (7)]. Similarly, for the spin-up left-movers, the Fermi level is then shifted to smaller momenta, where the $S_k^{r=L}$ suppress the interaction.²⁸ As a result, $\delta E(S)$ develops a minimum at $S = S_{\text{min}} < S_{\text{max}}$, and the system is stable there. Intuitively, this may be understood on the basis of a variational calculation (see Appendix A). Within exact diagonalization one finds that with $\Gamma_1 = 6/\pi$, the ground state degeneracy increases successively from 0 to $2S_{\text{max}} + 1$ by first adding the lowest energy eigenstates of the $S_z = \pm 1$ subspaces to the ground space, and then the $S_z = \pm 2$ subspaces and so forth. This is shown in Fig. 4 (b).

If the total spin S is plotted as a function of $v_F \pi / U$, S decreases from S_{max} to 0 in steps. These steps correspond to the positions $v_F \pi / U$, where the degree of the ground state degeneracy changes, indicated by arrows in Fig. 4. For $\Gamma_1 = 0$, there is one step where the spin-polarization jumps from $S = S_{\text{max}} = N/2$ to $S = 0$, while for the maximal $\Gamma_1 = 6/\pi$, there are $N/4$ steps at each of which the spin-polarization is decreased by $\Delta S = 2$.²⁹ Fig. 5 shows these two limiting cases and how the steps evolve as Γ_1 is varied from 0 to $6/\pi$. The momentum-dependence must have a minimum strength

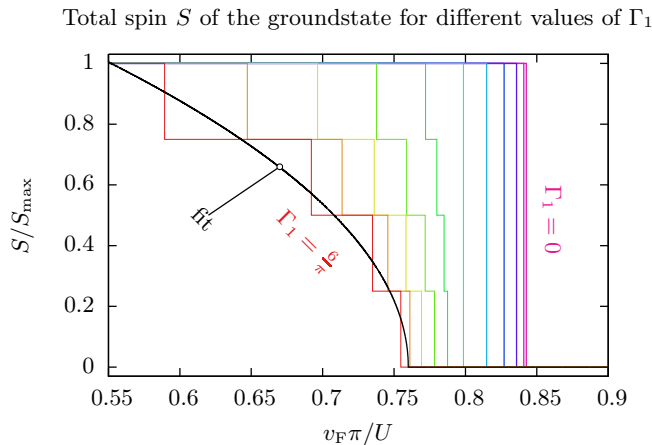


FIG. 5. (Color online) Dependence of the spin-polarization S on $v_F\pi/U$ for different strengths of the momentum-dependence Γ_1 from $\Gamma_1 = 0$ (rightmost curve) to $\Gamma_1 = \frac{6}{\pi}$ (leftmost curve) in steps of $\Delta\Gamma_1 = \frac{6}{10\pi}$. The length of the edge is $L = 48$, $\lambda_{bs} = 1$ and $\lambda_{us} = 0$. The smooth curve is a power law fit to the plateau centers of the $\Gamma_1 = \frac{6}{\pi}$ steps with exponent $\beta = 0.5$ (see text).

$\Gamma_1 > \Gamma_1^c \simeq 1$, in order to break the one big spin-polarization step of height $N/2$ into many small steps of height 2. Thus, for $\Gamma_1 > \Gamma_1^c$ there is a regime of weak edge magnetism, meaning that the total spin S of the ground state is smaller than the maximal spin S_{\max} , in addition to the usual saturated edge magnetism for small $v_F\pi/U$ (i.e. $S = S_{\max}$) and the Luttinger liquid regime for large $v_F\pi/U$ with $S = 0$. Figure 6 shows a diagram in which the phase boundaries between the Luttinger liquid (LL), the saturated edge magnetism (SEM) and the novel weak edge magnetism (WEM) are shown for different system sizes $N = 8, 12, 16$.

Note that the non-zero Γ_1^c found in the exact diagonalization reveals a weakness of the fermionic mean-field theory in which this minimum momentum dependence, above which a WEM regime appears, is zero (see Appendix A). A non-zero Γ_1^c means that the small momentum-dependencies which always follow from a dependence of the Bloch wave functions in usual one-dimensional conductors on the momentum are not necessarily sufficient to stabilize the weak edge magnetism; the momentum-dependence of the interaction vertex must be sufficiently strong for this.

In the limit $L \rightarrow \infty$, which cannot be accessed within exact diagonalization, of course, S/S_{\max} becomes a smooth function of $v_F\pi/U$. We approximate this smooth function by a power law

$$S/S_{\max} \sim \left[\left(\frac{v_F\pi}{U} \right)_{\text{crit.}} - \frac{v_F\pi}{U} \right]^\beta. \quad (14)$$

Fermionic mean-field theory (see Appendix A) predicts $\beta = 0.5$. Because the exact diagonalization study is limited to small systems $N \leq 16$, it is difficult to obtain a

decent estimate of the exact exponent β within this work. Fitting the edge state limit of the generalized model to the center of the plateaus of the $N = 16$ results of the exact diagonalization, we obtain $0.44 < \beta < 0.61$, dependent on how many plateaus are included in the fit. The critical point $\left(\frac{v_F\pi}{U} \right)_{\text{crit.}} \simeq 0.760$ for this fit is obtained by extrapolating the rightmost step from the data sets $N = 4, 8, 12, 16$ to $N = \infty$.

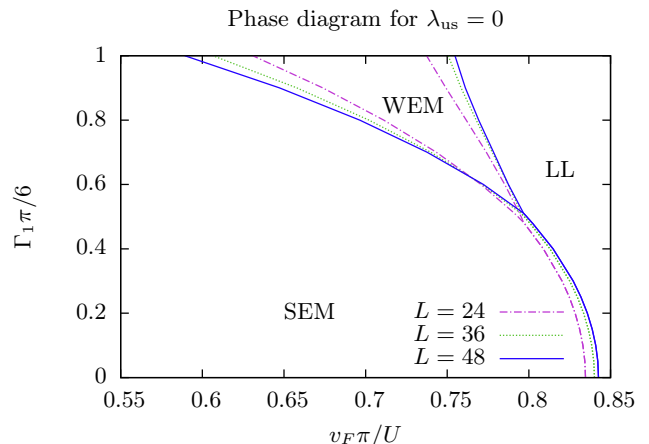


FIG. 6. (Color online) Phase diagram for lengths $L = 24$, $L = 36$ and $L = 48$. For small velocity dependence Γ_1 of the interaction, only the Luttinger liquid (LL) phase and the saturated edge magnetism (SEM) phase exist, whereas above the critical value of $\Gamma_1 = \Gamma_1^c$ the weak edge magnetism (WEM) phase appears.

Interestingly, Γ_1 not only affects the order of the transition but also the critical $v_F\pi/U$. This is also not correctly predicted by the mean-field approach (see Appendix A), which, independently of Γ_1 , finds $v_F\pi/U = 1$ to be the critical point. For small Γ_1 and $N = 16$ the exact diagonalization gives

$$\left[\frac{v_F\pi}{U} \right]_{\text{crit.}} \simeq 0.84 - 0.17\Gamma_1^2. \quad (15)$$

For the maximal $\Gamma_1 = 6/\pi$, the position of the leftmost step can be calculated by exact diagonalization for very large systems.¹⁸ We performed calculations for system sizes up to $L = 180$ in order to extrapolate this step position. Within the limits of the accuracy of this extrapolation, the critical point $v_F\pi/U = 0.5 \pm 0.001$ between the SEM and the WEM regime coincides with the mean-field prediction (see Appendix A). This extrapolation to the thermodynamic limit, in combination with the extrapolation of the critical point between the WEM and the LL regime, is a strong evidence for the existence of the WEM phase for $0.5 \leq v_F\pi/U \leq 0.760$ in the thermodynamic limit.

For completeness we note that our exact diagonalization analysis shows that a SEM phase also exists in the general model with umklapp scattering $\lambda_{us} = 1$ if $\Gamma_1 > 0$. However even for $\Gamma_1 = 6/\pi$ there is no weak edge mag-

netism phase between the Luttinger liquid and the saturated edge magnetism as long as $\lambda_{\text{us}} = 1$.

B. The relevance of backscattering

The backscattering Hamiltonian H_1^{bs} is important for the SU(2) invariance of the Hamiltonian. It is easily seen that only for $\lambda_{\text{bs}} = 1$ the SU(2) symmetry is preserved. At real graphene edges, of course, the backscattering cannot be tuned experimentally. Nevertheless it is interesting to study the consequences of a suppression of H_1^{bs} since in a bosonization treatment of the generalized model H_1^{bs} translates to a sine-Gordon term which is difficult to analyze. Therefore, some insight into the relevance of H_1^{bs} is helpful from a theoretical point of view. Following the philosophy of the previous subsection, we restrict the discussion to the spin polarization properties of the ground state. The analysis of more complicated observables such as spin-spin correlation functions is beyond the scope of this work and will be discussed in another paper.

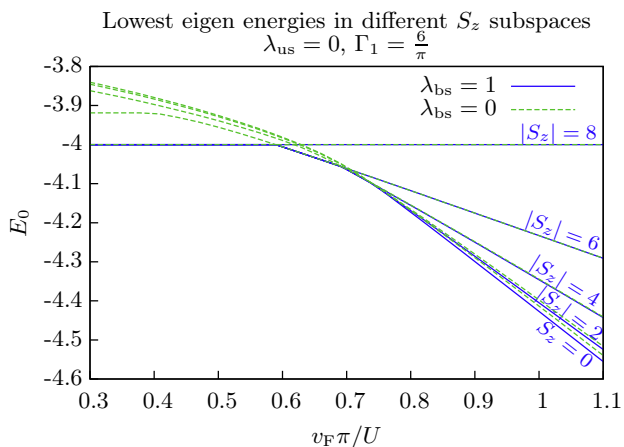


FIG. 7. (Color online) The lowest eigen energies of different S_z subspaces with (solid blue) and without (dashed green) backscattering calculated for an edge of length $L = 48$. The broken SU(2) symmetry in the case of $\lambda_{\text{bs}} \neq 1$ lifts the degeneracy of the ground states in the different S_z subspaces.

Fig. 7 compares the lowest eigen energies of the S_z subspaces from calculations with and without backscattering. The most striking feature of the suppression of backscattering is the lifting of the ground state degeneracy in the SEM regime. This effect is easily understood by noting that the very reason for the ground state degeneracy in the $\lambda_{\text{bs}} = 1$ case was the SU(2) symmetry, which, however, is broken for $\lambda_{\text{bs}} < 1$. Interestingly, the lifting of the degeneracy is such that the lowest energy states of the subspaces with highest $|S_z|$, in the ground space for $\lambda_{\text{bs}} = 1$, form the ground state for $\lambda_{\text{bs}} < 1$. This means that suppressing backscattering introduces an Ising anisotropy along the spin quantization axis cho-

sen in the definition of the model.

Apart from this degeneracy lifting, the evolution of the ground state properties with $v_F \pi / U$ is very similar for calculations with and without backscattering. The positions of the highest spin-polarization steps are practically unchanged. Only at the steps close to the phase transition between the LL and the WEM regime, a deviation of the $\lambda_{\text{bs}} = 0$ results from the $\lambda_{\text{bs}} = 1$ results can be observed. A handwaving explanation of this behavior can be given in terms of the bosonization analysis of the WEM regime in Ref. 13. As soon as the Fermi levels for the up-spin electrons and the down-spin electrons are split, the backscattering process for electrons right at the Fermi surface is forbidden because it is not momentum-conserving. Thus, in order to conserve momentum, the electrons are forced to scatter to higher energies if there is a non-zero spin-polarization. This mechanism suppresses the backscattering. In the bosonization language the backscattering Hamiltonian acquires a spatially oscillating phase which makes the corresponding operator irrelevant in the renormalization group. Thus in the WEM regime, not too close to the critical point, H_1^{bs} is suppressed and does not give an important contribution.

Close to the critical point, however, Fig. 7 indicates that H_1^{bs} becomes more important. This observation is consistent with the qualitative bosonization argument: Close to the critical point the phase oscillations in the bosonic backscattering Hamiltonian get slower until they completely disappear at the critical point.

IV. DISCUSSION

On the basis of a generalized class of effective models for one-dimensional interacting electrons we have studied the magnetic properties of a graphene zigzag edge. Using exact diagonalization we confirmed the existence of three phases within these models, namely the saturated edge magnetism phase which is present at normal graphene edges, the Luttinger liquid phase which appears for edge states with strongly enhanced bandwidth, and an intermediate regime of weak edge magnetism. The latter phase is a realization of a ferromagnetic Luttinger liquid, a one-dimensional itinerant ferromagnet. We presented evidence that the transition between the Luttinger liquid and the weak edge magnetism phase becomes a second order quantum phase transition in the limit of long edges.

Beyond the identification of the magnetic properties of edge states, we examined the question why electrons in one-dimensional edge states have such a rich phase diagram with two types of ferromagnetic ground states, while usual one-dimensional electrons do not show any ferromagnetism. In view of the Lieb-Mattis theorem,¹⁴ which actually forbids a spin-polarized ground state for interacting electrons in one dimension, this question becomes even more pressing.

A closer inspection of the edge state model, which was derived directly from the graphene crystal structure,¹³ revealed two unusual features of edge states which cannot be found in other one-dimensional electronic systems, such as quantum wires, for instance. These are (a) the total absence of umklapp processes in the effective electron-electron interaction, independently of the filling factor, and (b) a strong momentum dependence of the effective interaction vertex. Each of these features precludes the applicability of the Lieb-Mattis theorem. The momentum-dependence gives rise to a complicated non-local interaction, which cannot be written as $V(x, y)\hat{n}(x)\hat{n}(y)$, with $\hat{n}(x)$ an electron density operator, as it is required for the Lieb-Mattis theorem. And even in the limit of momentum-independent interactions ($\Gamma_1 = 0$ in the general model) the suppressed umklapp scattering makes the reformulation as a density-density interaction in real space impossible. In order to further track down the particular consequences of these special features for the magnetic properties of graphene edges, we replenished the direct model with a tunable umklapp scattering term and replaced the interaction vertex by a generalized vertex function in which the momentum-dependence can be switched on and off.

The study of this generalized model, which can be tuned continuously between its edge state limit and a regime in which it describes normal one-dimensional metals, revealed the significance of the two edge state features: the absence of umklapp processes is responsible for the existence of a spin-polarized ground state, and the strong momentum dependence of the interaction vertex stabilizes a regime of weak edge magnetism and gives rise to a second order phase transition between the paramagnetic Luttinger liquid and the ferromagnetic Luttinger liquid.

It is interesting to note that the stabilization of the weak edge magnetism phase seems to be very robust against changes in the details of the interaction vertex function. Apparently it is only important that the vertex is suppressed as one of the four momenta of the participating fermions gets close to one of the Dirac points. The exact functional form of this suppression, however, seems to be irrelevant, since the qualitative behavior of the spin-polarization did not depend on whether we used the interaction vertex of the direct model or the interaction vertex of the generalized model with maximal momentum dependence. These two vertex functions have in common that they vanish as one of the momenta approaches a Dirac point. However, their functional forms are very different.

Finally we note that one-dimensional itinerant magnetism has also been studied in Hubbard chains with an additional second neighbor hopping,^{30,31} showing that it is indeed possible to define one-dimensional models which, at first sight, seem to comply with the prerequisites of the Lieb-Mattis theorem, but nevertheless have a high spin ground state. The physical picture behind the model discussed in Refs. 30 and 31, however, is much

different from the present work. Interestingly, the sign of the hopping amplitude to the nearest neighbor must be different from the sign of the next-nearest neighbor hopping for the system to have a ferromagnetic ground state.

Also, we emphasize that the model discussed here is the low-energy theory of a realistic system which may be studied experimentally. It has been derived in direct line from a two-dimensional lattice model of graphene/graphane interfaces.^{13,20}

ACKNOWLEDGMENTS

D.J.L. and F.F.A. acknowledge financial support from the DFG for grant AS120/4-3. M.J.S. acknowledges financial support from the Swiss NSF and from the NCCR QSIT.

Appendix A: Variational analysis of the generalized model

We calculate the magnetic ground state properties of the generalized model within a fermionic mean-field approximation. It is assumed that only the averages $\langle c_{kr\sigma}^\dagger c_{kr\sigma} \rangle$ are non-zero, so that the umklapp Hamiltonian H_1^{us} and the backscattering Hamiltonian H_1^{bs} drop out of the mean-field treatment. The resulting non-interacting Hamiltonian is diagonal in the momentum k , in the direction of motion r and in the z -spin projection, so that the mean-field theory is equivalent to a variational ansatz based on the trial wave function

$$|M\rangle = \prod_{\sigma} \left[\prod_{k < k_{F\sigma}} c_{kR\sigma}^\dagger \right] \left[\prod_{k > -k_{F\sigma}} c_{kL\sigma}^\dagger \right] |0\rangle \quad (\text{A1})$$

with an asymmetric occupation of spin-up and spin-down states. The variational parameter $M \in [0, 1]$ is related to the spin-dependent Fermi levels by

$$k_{F\sigma} = \sigma \frac{\pi}{6} M, \quad (\text{A2})$$

and to the spin-polarization S , used in Sect. III, by $M = S/S_{\text{max}}$. For finite size systems, as discussed in the main part of this paper, the Fermi level cannot be varied continuously so that also M is a discrete variable in this case. However, within mean-field theory it is easy to perform the calculations in the thermodynamic limit, so that we will consider M to be a continuous variable and interpret it as the magnetization order parameter.

The variational energy $E(M)$ is easily calculated from the Hamiltonian H in Eq. (11)

$$E(M) = \langle M | H | M \rangle = \frac{1}{36}(\pi v_F - U)M^2 + \Gamma_1^2 \frac{U\pi^2}{5184} M^4. \quad (\text{A3})$$

For $U < \pi v_F$, the minimum of $E(M)$ is at $M = 0$, while for $U > \pi v_F$ the mean-field ground state has a finite magnetization

$$M = \min \left[\frac{\sqrt{72}}{\pi\Gamma_1} \sqrt{1 - \frac{v_F\pi}{U}}, 1 \right] \quad (\text{A4})$$

Note that by definition the magnetization cannot become larger than 1. From Eq. (A4) it becomes obvious that a non-zero momentum-dependence Γ_1 is required to stabilize the regime of weak edge magnetism. For $\Gamma_1 = 0$, the magnetization would jump from 0 to 1 at the critical point $U = v_F\pi$.

The existence of the weak edge magnetism can be traced back to the M^4 term in Eq. (A3) which is generated by the momentum-dependence Γ_1 of the interaction vertex. In dimensions higher than one, such M^4 terms emerge also from momentum-independent interactions or directly from the kinetic energy, so that at least on the mean-field level $\Gamma_1 > 0$ is required for the stabilization of weak ferromagnetism only in one dimension.

Appendix B: Exact diagonalization of the direct model

The direct model Hamiltonian H^{dm} defined by Eqs. (3 - 4) and the edge state limit of the generalized model Hamiltonian H [Eq. (11) with $\lambda_{\text{bs}} = 1$, $\lambda_{\text{us}} = 0$ and $\Gamma_1 = 6/\pi$] are not exactly equal, as the general model linearizes the single particle dispersion and replaces the factors \mathcal{N}_p by the approximation S_k^r . Nevertheless, the most important properties of graphene edge states, i.e. the momentum-dependence of the interaction vertex and the absence of umklapp scattering, are properly described by both, the direct model and the general model in the edge state limit.

In this appendix, we check that the direct model has qualitatively the same magnetic properties as the general model in the edge state limit. In Fig. 8, we present the spin-polarization S as a function of Δ/U , obtained from the exact diagonalization of the direct model. The bandwidth parameter Δ of the direct model corresponds to the Fermi velocity v_F of the general model.

Clearly, for larger Δ/U , which corresponds to the parameter $v_F\pi/U$ in the generalized model, we obtain a Luttinger liquid phase with a ground state of total spin $S = 0$. An intermediate regime with weak edge magnetism exists, where the total spin of the ground state $S < S_{\text{max}}$ is not maximal. As in the exact diagonalization analysis of the general model in the main text, only some of the lowest eigen energies in different S_z subspaces are degenerate and form the ground state. For small Δ/U , the saturated edge magnetism phase is reached and the spin of the ground state is maximal, i.e., the lowest eigen energies in *all* S_z subspaces are degenerate.

Note that the energy of the fully spin polarized eigenstate of the direct model Hamiltonian has a finite slope

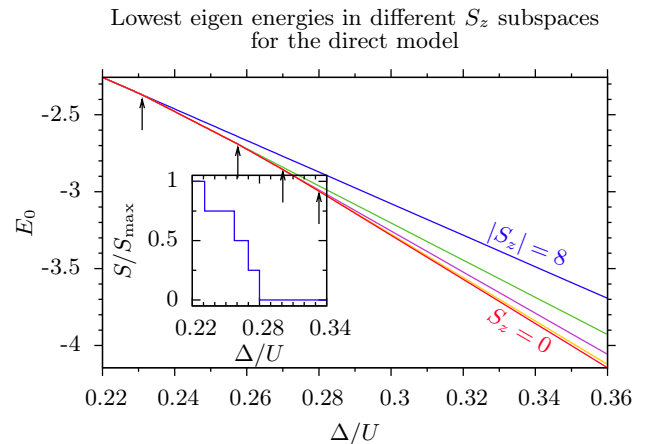


FIG. 8. (Color online) Lowest eigen energies in the $S_z = 0, \pm 2, \pm 4, \pm 6, \pm 8$ subspaces (from bottom to top) for the direct model calculated for an edge of length $L = 48$. The inset shows the dependence of the spin-polarization S as a function of Δ/U determined from the degeneracy of the ground state.

(see Fig. 8). This is because the direct model lacks a symmetry of H_0 of the generalized model leading to $E_0^{S_{\text{max}}}(v_F) = \text{const}$ (cf. Fig. 4). As only the degeneracy of the lowest eigen energies are important, but not their absolute values, this difference does not have any physical consequences.

¹ K. S. Novoselov, A. K. Geim, S. V. Morozov, D. Jiang, Y. Zhang, S. V. Dubonos, I. V. Grigorieva, and A. A. Firsov, *Science* **306**, 666 (2004).
² A. H. Castro Neto, F. Guinea, N. M. R. Peres, K. S. Novoselov, and A. K. Geim, *Rev. Mod. Phys.* **81**, 109 (Jan 2009).
³ C. Lee, X. Weil, J. W. Kysar, and J. Hone, *Science* **321**, 385 (2008).
⁴ Y. Zhang, Y.-W. Tan, H. L. Stormer, and P. Kim, *Nature* **438**, 201 (Nov 2005), ISSN 0028-0836, <http://dx.doi.org/10.1038/nature04235>.

⁵ K. S. Novoselov, A. K. Geim, S. V. Morozov, D. Jiang, M. I. Katsnelson, I. V. Grigorieva, S. V. Dubonos, and A. A. Firsov, *Nature* **438**, 197 (Nov 2005), ISSN 0028-0836.
⁶ M. Fujita, K. Wakabayashi, K. Nakada, and K. Kusakabe, *Journal of the Physical Society of Japan* **65**, 1920 (1996), <http://jpsj.ipap.jp/link?JPSJ/65/1920/>.
⁷ Y.-W. Son, M. L. Cohen, and S. G. Louie, *Phys. Rev. Lett.* **97**, 216803 (Nov 2006).
⁸ Y.-W. Son, M. L. Cohen, and S. G. Louie, *Nature* **444**, 347 (2007).

- ⁹ J. Jung and A. H. MacDonald, Phys. Rev. B **79**, 235433 (Jun 2009).
- ¹⁰ H. Feldner, Z. Y. Meng, A. Honecker, D. Cabra, S. Wessel, and F. F. Assaad, Phys. Rev. B **81**, 115416 (Mar 2010).
- ¹¹ H. Feldner, Z. Y. Meng, T. C. Lang, F. F. Assaad, S. Wessel, and A. Honecker, “Dynamical signatures of edge-state magnetism on graphene nanoribbons,” (2011), arXiv:1101.1882.
- ¹² T. Hikihara, X. Hu, H.-H. Lin, and C.-Y. Mou, Phys. Rev. B **68**, 035432 (Jul 2003).
- ¹³ M. J. Schmidt and D. Loss, Phys. Rev. B **82**, 085422 (Aug 2010).
- ¹⁴ E. Lieb and D. Mattis, Phys. Rev. **125**, 164 (Jan 1962).
- ¹⁵ C. Lanczos, J. Res. Nat. Bur. Stand. **45**, 255 (1950).
- ¹⁶ E. Dagotto, Rev. Mod. Phys. **66**, 763 (Jul 1994).
- ¹⁷ D. Sénéchal, “An introduction to quantum cluster methods,” (2008), arXiv:0806.2690v2.
- ¹⁸ At $L/3$ filling, and $S_z = 0$, we could access edges of length $L = 48$ with a dimension of the corresponding Hilbert space of 2 594 212 after exploiting all symmetries. For nearly maximal $S_z = L/6 - 2$ and $L/3$ filling, we were able to calculate the groundstate energy of an edge with length $L = 180$ with a Hilbert space dimension of only 26 580. In this case we were limited only by the 64 bit limit of the internal storage of the basis vectors and longer edges are in principle accessible by a modification of our code.
- ¹⁹ It is only important to assume that this energy scale is large enough so that the restriction to the zero energy sector of \mathcal{H} is well justified. The validity of this assumption has been checked in Ref. 13.
- ²⁰ M. J. Schmidt and D. Loss, Phys. Rev. B **81**, 165439 (Apr 2010).
- ²¹ M. Hohenadler, T. C. Lang, and F. F. Assaad(2011), arXiv:1011.5063.
- ²² T. Giamarchi, *Quantum Physics in One Dimension* (Oxford Univ. Press, 2003).
- ²³ The equal strength of the g_2 and g_4 processes is due to the symmetry property $\Gamma(-k_F, k_F, 2k_F) = \Gamma(\pm k_F, \pm k_F, 0)$, which is a consequence of the origin of Γ in the 2D honeycomb Hubbard model (see Ref. 13).
- ²⁴ M. J. Schmidt(2011).
- ²⁵ An edge with L unit cells in length corresponds to only $L/3$ k-space points in the reduced Brillouin zone in which the edge states are defined.
- ²⁶ We have checked that the linearization of the single particle spectrum does not change the results qualitatively.
- ²⁷ The point $v_F \pi / U = 0$ corresponds to a *pathologic potential* in Ref. 14, as it can be reached by $U \rightarrow \infty$. At this point, all sectors with total spin $0 \leq S \leq S_{\max}$ are degenerate.
- ²⁸ Note that the increase in the interaction vertex for the spin-down electrons with lowered Fermi level is overcompensated by the suppression due to the higher Fermi level of the spin-up electrons, so that in total the interaction is reduced as S grows.
- ²⁹ This decrease of 2 in S is due to the contribution of the left- and right-moving branch to the spin-polarization: each branch contributes one spin flip.
- ³⁰ S. Daul, Eur. Phys. J. B **14**, 649 (2000).
- ³¹ S. Daul and R. M. Noack, Phys. Rev. B **58**, 2635 (1998).